nature physics

LETTERS

https://doi.org/10.1038/s41567-018-0262-1

Collective mechanical adaptation of honeybee swarms

O. Peleg[1,4], J. M. Peters[2,4], M. K. Salcedo[2] and L. Mahadevan[1,2,3*]

Honeybee *Apis mellifera* swarms form large congested tree-hanging clusters made solely of bees attached to each other[1]. How these structures are maintained under the influence of dynamic mechanical forcing is unknown. To address this, we created pendant clusters and subject them to dynamic loads of varying orientation, amplitude, frequency and duration. We find that horizontally shaken clusters adapt by spreading out to form wider, flatter cones that recover their original shape when unloaded. Measuring the response of a cluster to an impulsive pendular excitation shows that flattened cones deform less and relax faster than the elongated ones (that is, they are more stable). Particle-based simulations of a passive assemblage suggest a behavioural hypothesis: individual bees respond to local variations in strain by moving up the strain gradient, which is qualitatively consistent with our observations of individual bee movement during dynamic loading. The simulations also suggest that vertical shaking will not lead to significant differential strains and thus no shape adaptation, which we confirmed experimentally. Together, our findings highlight how a super-organismal structure responds to dynamic loading by actively changing its morphology to improve the collective stability of the cluster at the expense of increasing the average mechanical burden of an individual.

Collective dynamics allow super-organisms to function in ways that a single organism cannot, by virtue of their emergent size, shape, physiology and behaviour[2]. Classic examples include the physiological and behavioural strategies seen in social insects (for example, ants that link their bodies to form rafts to survive floods[3–6], assemble pulling chains to move food items[7], and form bivouacs[8] and towers[9], as well as bridges and ladders to traverse rough terrain[10]). Similarly, groups of `daddy longlegs' (order Opiliones) huddle together and emperor penguins cluster together for thermoregulation purposes[11]. While much is known about the static forms that are seen in such situations, the stability of these forms to dynamic perturbation, and their global adaptation to environmental changes is much less understood.

European honeybees, *Apis mellifera* L., show many of these collective behaviours during their life cycle[1]. For example, colonies reproduce through colony fission, a process in which a subset of the colony's workers and a queen leave the hive, separate from the parent colony and form a cluster on a nearby tree branch[1]. In these swarm clusters (which we will refer to as clusters), the bees adhere to each other and form a large structure made of ~10,000 individuals and hundreds of times the size of a single organism (Fig. 1a). Generally, this hanging mass of adhered bees takes on the shape of an inverted pendant cone; however, the resultant shape is also influenced by the surface to which the cluster is clinging to (see two different examples in Fig. 1a). The cluster can stay in place for several days as scout bees search the surrounding area for suitable nest sites[1].

The colony is exposed to the environment during this stage and shows several behaviours to cope with the fluctuating thermal and mechanical environment. For instance, clusters tune their density and surface area to volume ratio to maintain a near constant core temperature despite large fluctuations in the ambient temperature[12–14]. Furthermore, at high temperatures, the swarm expands and forms channels that are presumed to aid in air circulation[12]. Moreover, in response to rain, bees at the surface arrange themselves to form `shingles', shedding moisture efficiently from the surface of the cluster[15]. Similarly, the cluster is mechanically stable; while it sways from side to side in the wind (for example, see Supplementary Video 1), it could be catastrophic if the cluster breaks (when a critical load occurs) as the bees would lose the ability to minimize surface area to prevent hypothermia, while still being mechanically stable. However, the mechanism by which a multitude of bees work together to create and maintain a stable structure that handles both static gravity and dynamic shaking stimuli (for example, wind and predators) remains elusive. To understand this, we develop a laboratory experimental set-up, for ease of visualization and manipulation, to quantify the response of a honeybee cluster to mechanical shaking over short and long times.

To prepare a cluster, we attach a caged queen (see Supplementary Section A) to a board and allowed a cluster to form around her (Fig. 1b). The bees at the base grip onto an area that is roughly circular. The board is controlled by a motor that can produce movement in the horizontal direction at different frequencies (0.5–5 Hz) and accelerations (ranged 0–0.1g). We apply both discontinuous shaking in which the acceleration is kept constant and the frequency is modified, and vice versa, continuous shaking in which the frequency is kept constant and the acceleration is modified (see Supplementary Fig. 2).

For the case of horizontal shaking (for both discontinuous and continuous), the tall conical cluster swings to and fro in a pendular mode (one of the lowest energy modes of motion, see Supplementary Section C), with a typical frequency of ~1 Hz. However, over longer durations (that is, minutes), the bees adapt by spreading themselves into a flatter conical form (Fig. 1b–d and Supplementary Video 2), while their total number remains constant (measured by the total weight of the cluster). The final shape flattens as the shaking continues for longer, or as the frequency and acceleration of shaking increases. For the discontinuous shaking, when we plot the relative extent of spreading (scaled by a constant) as measured by $A(t)/A(0)$ for all different frequencies, as a function of number of shakes, the data collapse onto a single curve (Fig. 2a). This suggests that the

[1]Paulson School of Engineering and Applied Sciences, Harvard University, Cambridge, MA, USA. [2]Department of Organismic and Evolutionary Biology, Harvard University, Cambridge, MA, USA. [3]Department of Physics, Kavli Institute for NanoBio Science and Technology, Harvard University, Cambridge, MA, USA. [4]These authors contributed equally: O. Peleg, J. M. Peters. *e-mail: lmahadev@g.harvard.edu

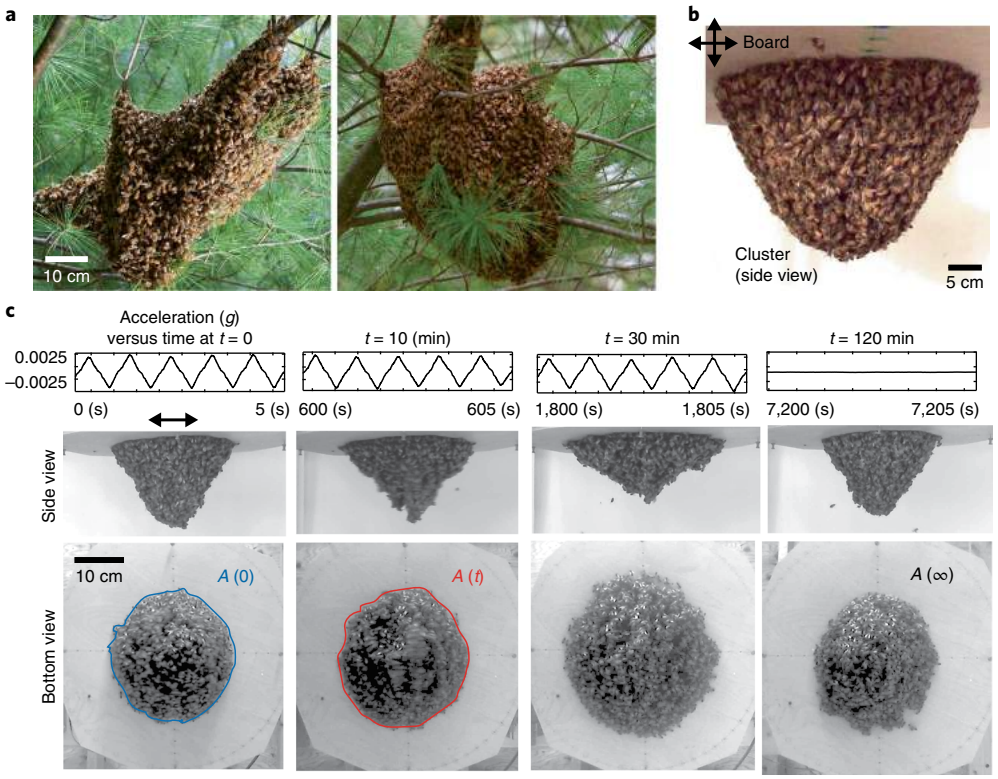

Fig. 1 | A mechanically adaptive honeybee cluster. a, Bee clusters on a tree branch. **b**, The experimental set-up consists of a motor driving a wooden board, on which a cluster of bees grips a roughly circular contact area. The motor can produce periodic movement in the horizontal or vertical axis at different frequencies and amplitudes. See Supplementary Fig. 1 for the full set-up. **c**, The top panel shows the acceleration of the board versus time. The middle and bottom panels show how the bee cluster adapts its shape dynamically: elongated cluster at $t=0$ (left column), spread-out cluster after horizontal shaking for 10 min and 30 min (middle columns), and elongated cluster after relaxation (right column); side and bottom views. The contact area before and after shaking is highlighted in blue and red, respectively.

cluster response scales with both the number and magnitude of shakes, but over much longer timescales than an individual event. The nature of this response is independent of the type of stimulus: when the shaking signal is continuous, we see a similar response (Fig. 2b). The graded adaptive response that scales with the number of shakes and is a function of applied displacements and frequencies, and the absence of any adaptation to very low frequencies and amplitudes (orange curves in Fig. 2b), suggests that there is a critical relative displacement (that is, a threshold mechanical strain) needed to trigger this adaptation. Once the shaking stops, the cluster returns to its original elongated cone configuration over a period of 30–120 min, a time that is much larger than the time for the cluster to flatten. This reversible cluster shape change in response to dynamic loading might be a functional adaptation that increases the mechanical stability of a flattened cluster relative to an elongated one.

To explore this suggestion quantitatively, we first define a laboratory-fixed coordinate system with axes as shown in Fig. 2c, with respect to which the board is at $\mathbf{r}_b(t)=[U_b, 0, W_b]$, the position of a bee i is defined as $\mathbf{r}_i(t)=[X_i(t), Y_i(t), Z_i(t)]$ and its displacement is defined as $[U_i(t), 0, W_i(t)]=\mathbf{r}_i(t)-\mathbf{r}_i(0)-\mathbf{r}_b(t)$. This allows us to track individual bees[16] along the surface of the cluster along the centreline $X_i(0)=0$ (Fig. 2d and Supplementary Video 3), over a period of oscillation. Comparing trajectories of bees in an elongated cluster and a flat cluster (that is, before and after shaking) shows that relative displacement between the bees at the cluster tip and bees at the base is significantly larger for an elongated cluster. Snapshots of tracked bees highlight the decoupling of movement of the tip and base of the cluster; that is, local deformations such as normal and shear strains are reduced in the mechanically adapted state corresponding to a spread cluster. A similar trend is observed when the cluster is subjected to a single sharp shake (see signal at Supplementary Fig. 2c), as shown in Supplementary Video 4. These measurements confirm that the adapted flattened structure is indeed more mechanically stable in the presence of dynamic horizontal loads.

The spreading of the cluster is a collective process, begging the question of how this collective spreading behaviour is achieved. To study this, we tracked bees on the surface of the cluster during the process of adaptive spreading, particularly at the early stages. In Fig. 2e and Supplementary Video 5, we show how bees move from the tip regions that are subject to large relative displacements towards the base regions that are subject to small relative displacements. This suggests a simple behavioural law wherein the change in relative displacement U_i between neighbouring bees is a driver of shape adaptation: individual bees sense the local deformation relative to their neighbours and move towards regions of lower U_i (illustrated in Fig. 2f). In the continuum limit, this corresponds to their ability to sense strain gradients, and move from regions of lower strain (near the free tip) towards regions of higher strain (near the fixed base). It is worth noting here that this behavioural law is naturally invariant to rigid translation and rotation of the cluster, and thus depends only on the local mechanical environment each bee experiences.

However, what measure of the relative displacements might the bees be responding to? To understand this, we note that the fundamental modes[17] of a pendant elastic cone are similar to those of a pendulum swinging from side to side, and a spring bouncing up and down, and their frequencies monotonically increase as a function of the aspect ratio of the cluster (Supplementary Fig. 3; see Supplementary Section C for details). To quantify the deviations

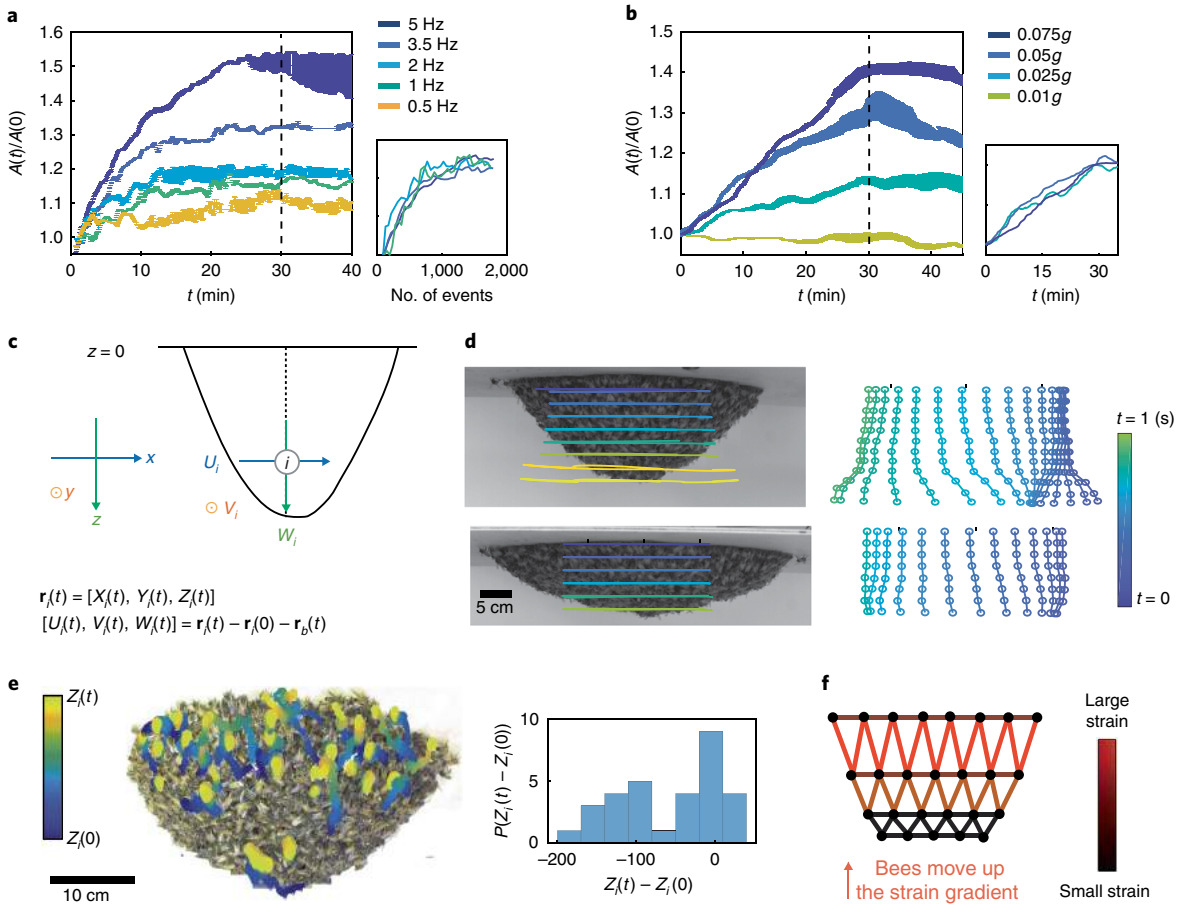

Fig. 2 | Quantifying adaptive response of the cluster to horizontal shaking. For all shaking frequencies, the base contact area of the cluster increases monotonically until a plateau is reached. Once shaking ceases, the cluster responds by gradually reverting to its original shape by increasing its contact area, but at a much slower rate. **a**, Ratio of the contact area of the base of the cluster divided by its original area $A(t)/A(0)$ as a function of time, for the discontinuous case. The colours represent results for different frequencies of periodic shaking. The inset shows that the scaled base area collapses onto a master curve when plotted versus the number of shaking events. The error bars correspond to the standard deviation of three individual trials (see Supplementary Table 1 for more information about trial repetitions). **b**, $A(t)/A(0)$ for continuous shaking shows the same qualitative behaviour; note that when the acceleration is very small ($0.01g$), there is no response (that is, there is a critical threshold of forcing below which the bees do not respond). **c**, Coordinate systems of the laboratory frame and the displacement coordinates of the individual bees. **d**, Deformation of an elongated cluster before shaking began ($t=0$, top) and a flattened cluster after shaking ($t=30$ minutes, bottom) shows that displacement at the tip of the cluster is largest. On the right: time snapshots of a string of bees along the centre of the cluster (see Supplementary Video 3). **e**, Trajectories of individual bees during 5 min of horizontal shaking show that when the cluster spreads out, surface bees move upwards. Colour code represents time: the trajectory starts with blue and ends with yellow. Inset: probability distribution function of vertical displacement, showing a net upward trend. **f**, An illustration of the behavioural constitutive law: bees sense the local deformation of connections to their newest neighbours; once the relative deformation reaches a critical value, the bees move up the gradient in relative deformation.

from this simple picture due to the particulate nature of the assemblage, we turn to a computational model of the passive dynamics of a cluster and explore the role of shape on a pendant mechanical assemblage of passive particles used to mimic bees. We model each bee in the cluster as a spherical particle that experiences three forces: a gravitational force, an attractive force between neighbouring particles, and a force that prevents inter-particle penetration (see Supplementary Section C for further details). The bees at the base are assumed to be strongly attached to the supporting board, and those on the surface are assumed to be free. To study the passive response of the entire system, the board is oscillated at different frequencies and amplitudes, while we follow the displacement of individual particles, $U_i(\mathbf{r}_i)$, as well as the relative displacement between neighbouring bees $\mathbf{l}_{ij}(t)=\mathbf{r}_i(t)-\mathbf{r}_j(t)$ (Fig. 3a). Decomposing the vector $\mathbf{l}_{ij}(t)$ into its magnitude and direction allows us to define two local deformation measures associated with the local normal strain and shear strain. The local dynamic normal strain associated with a particle (bee) i relative to its extension at $t=0$ is defined as $\delta l_i=\langle \max_{0\le t\le T} ||\mathbf{l}_{ij}(t)|-|\mathbf{l}_{ij}(0)|| \rangle$, where T is the duration from the onset of the applied mechanical shaking until the swarm recovers its steady-state configuration, and the angle brackets represent the average over all bees j that are connected to bee i. The local shear strain is calculated from the changes in the angle $|\angle(\mathbf{l}_{ij}(t),\mathbf{l}_{ik}(t))|$ between $\mathbf{l}_{ij}(t)$ and $\mathbf{l}_{ik}(t)$, connecting bees i and j, and bees i and k, respectively, with the shear strain, $\delta\theta_i$ defined as $\delta\theta_i=\langle \max_{0\le t\le T} |\angle(\mathbf{l}_{ij}(t),\mathbf{l}_{ik}(t))-\angle(\mathbf{l}_{ij}(0),\mathbf{l}_{ik}(0))| \rangle$, where the angle brackets represent the average over all pair of bees j–k that are connected to bee i.

As expected, we see that for the same forcing, the maximum amplitude of the local strains increases as the cluster becomes more elongated (Fig. 3a,b and Supplementary Video 6). Therefore, these local strains can serve as a signal for the bees to move, and a natural hypothesis is that once the signal is above a certain critical value, the bees move. However, how might they chose a direction? While

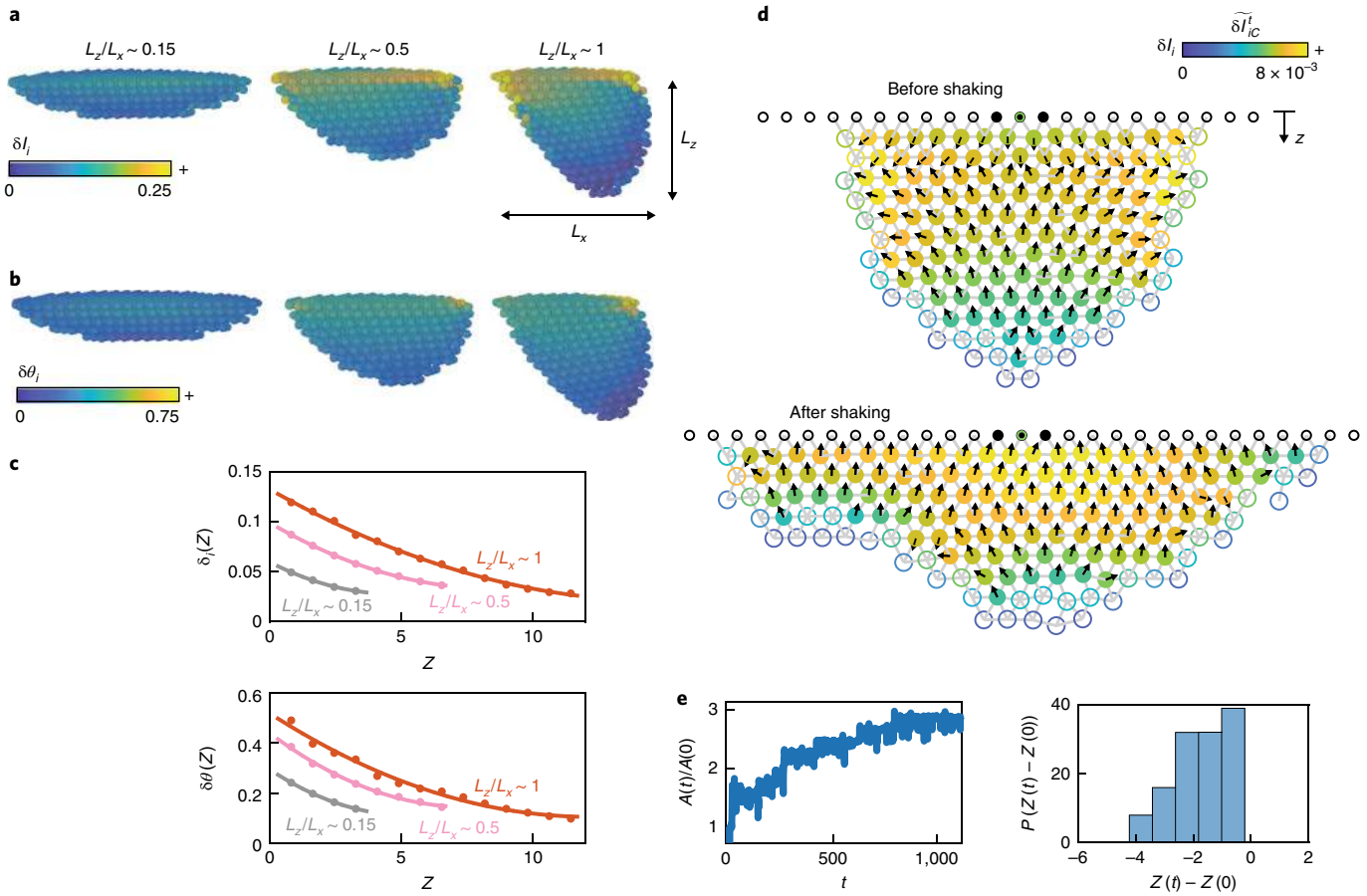

Fig. 3 | Computational model of mechanical adaptation. A cluster is modelled using particles that are linked via springs in a simple triangular lattice. **a**, Passive simulations: clusters of different aspect ratios (L_z/L_x), shown at the extreme of a period of horizontal oscillation. The colours represent the local normal strain of each honeybee δl_i, as defined in the text. Elongated clusters (on the right) experience a larger deformation at the tip of the cluster, while flattened clusters (on the left) experience much less deformation. **b**, For the same state as in **a**, we also show the maximum shear strain, $\delta\theta_i$. **c**, Plots of the mean normal and shear strain ($\delta l(Z)$ and $\delta\theta(Z)$) as a function of the distance from the base, Z, and aspect ratio L_z/L_x. We see that the maximum magnitude of the strains decreases as the cluster becomes flattened. **d**, Active stochastic simulations: when we impose a behavioural rule that allows the bees to sense the strains around them and move in the direction of increasing strain when the magnitude crosses a threshold ($\delta\tilde{l}^t_{iC}$), this leads to spreading. The colours represent the local integrated signal, $\delta\tilde{l}^t_i$, and the arrows point towards higher local signal. **e**, The scaled base contact area $A(t)/A(0)$ as a function of time, with the probability distribution function of vertical displacement, shows a net negative response (that is, bees move upwards on average), similar to experimental observations (see Fig. 2e).

it may be plausible for the bees to simply move upwards against gravity, it is probably difficult to sense a static force (that is, gravity) when experiencing large dynamic forcing (that is, shaking) in a tightly packed assemblage. Instead, we turn to ask whether there are any local signals that would give honeybees a sense of direction. For all clusters, the strains are largest near the base (Fig. 3a,b and Supplementary Video 6) and decrease away from it, but in addition, as the cluster becomes more elongated, there are large local strains along the contact line where $x = \pm L_1/2$, where the bees are in contact with the baseboard. This is due to the effect of the pendular mode of deformation that leads to rotation-induced stretching in these regions. To quantify how the normal and shear strain vary as a function of the distance from the base, Z, we average δl_i and $\delta\theta_i$ over all bees that were at a certain Z position at $t = 0$ and define the following mean quantities: $\delta l(Z) = \langle \delta l_i \rangle$, and $\delta\theta(Z) = \langle \delta\theta_i \rangle$, where the angle brackets indicate the average overall spring connection at the vertical position $r^i_z(0) = Z$. Similar to the experimental data, the simulations show that the displacements U_i for horizontal shaking of elongated clusters are larger in comparison to flattened clusters. As both strains $\delta l(Z)$ and $\delta\theta(Z)$ are largest near the base, $z = 0$ (Fig. 3c and Supplementary Video 6), and decrease away from the supporting baseboard, they may serve as local signals that bees at the tip of the cluster respond to by moving up the strain gradient (Supplementary Figs. 3–5 and Supplementary Videos 7 and 8).

This passive signature of a horizontally shaken assemblage suggests a simple behavioural hypothesis: bees can sense the local variations in the normal strain above a critical threshold, and move slowly up gradients collectively. We note that mechanical strain is invariant to translation and rotation of the whole assemblage; that is, it is independent of the origin and orientation of the frame of reference, and thus a natural choice (similar to how cells and bacteria respond to mechanical stresses[18]). This behaviour will naturally lead to spreading of the cluster and thence smaller strains on the cluster. Noting that the timescale of the response of the bees is of the order of minutes while the duration of a single period is seconds, it is natural to consider the integrated local normal strain signal: $\delta\tilde{l}^t_i = \sum^t_{\tilde{t}=t-T_w} \delta l^{\tilde{t}}_i \times \mathrm{d}t$, where T_w is chosen to be the period of the shaking (see detailed description in Supplementary Section C). Then our behavioural hypothesis is that when $\delta\tilde{l}^t_i > \delta\tilde{l}^t_{iC}$ the bee becomes active, and moves in the direction of the time-integrated negative normal strain gradient (that is, the active force is directed

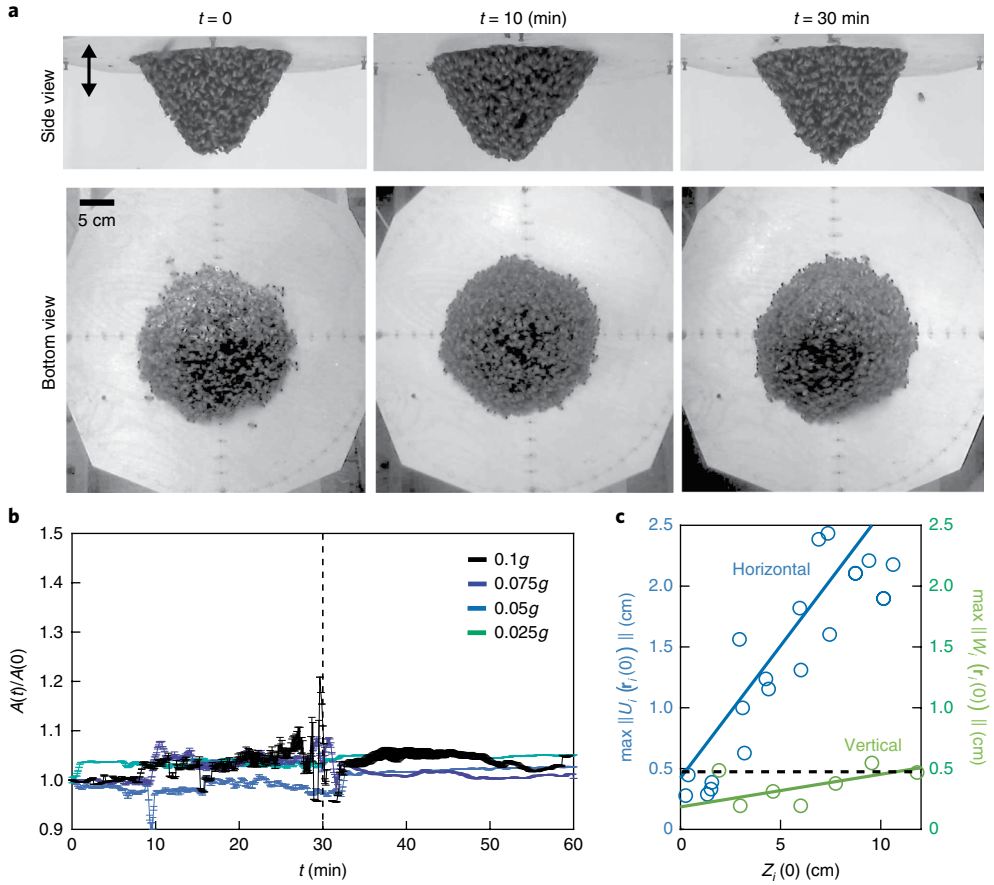

Fig. 4 | Response to vertical shaking. a, Vertical shaking (maximum acceleration 0.05*g*) of the bee cluster leads to a very small displacement. This is consistent with our simulations (see Supplementary Fig. 4 and Supplementary Section D) that vertical shakes do not destabilize the bees differentially. **b**, Contact area of the base of the cluster relative to its initial area $A(t)/A(0)$ versus time. Areas are defined as in Fig. 1d. The colours represent results for different accelerations of continuous shaking. **c**, Maximum displacement at the tip of a tall cluster as a result of a single horizontal and vertical shake. Bees do not respond or change the shape of the cluster when subjected to vertical shaking (green), but do respond substantially when shaken horizontally (blue). The black dotted line represents the experimentally observed threshold value to initiate active behaviour.

toward a higher local normal strain) according to the simple proportional rule $F^{\text{active}} = -f^{\text{active}}\widetilde{\delta \mathbf{l}}_i^t$. We note that moving up a gradient in time-integrated normal strain would also suffice to explain the observed mechanical adaptation.

We carry out our simulations of the active cluster in two dimensions for simplicity and speed (we do not expect any changes in three dimensions), allowing bonds to break and reform on the basis of proximity, similar to how bees form connections, and follow the shape of the cluster while it is shaken horizontally. We find that over time, the cluster spreads out to form a flattened cone (Fig. 3d,e and Supplementary Video 7), confirming that the local behavioural rule that integrates relative displacements that arise due to long-range passive coupling in the mechanical assemblage wherein bees actively move up the local gradient in normal strain δl_i is consistent with our observations.

If sufficiently large dynamic normal strain gradients drive shape adaptation, different shaking protocols that result in lower local strains should limit adaptation. One way is to shake the cluster gently, and this indeed leads to no adaptation (Fig. 2b responding to 0.01*g*). Another way to test our hypothesis is to shake the cluster vertically, exciting the spring-like mode of the assemblage. For the same range of amplitudes and frequencies as used for horizontal shaking, our simulations of a passive assemblage show that vertical shaking results in particles being collectively displaced up and down, with little variations in normal strain. As expected, even in active clusters with the behavioural rule implemented, little or no adaptation occurs as the threshold normal strain gradient is not achieved (Supplementary Figs. 5 and 6 and Supplementary Video 8). To test this experimentally, we shake the cluster vertically. We see that, in this case, the cluster shape remains approximately constant (Fig. 4a,b) until a critical acceleration is reached, at which time a propagating crack results in the detachment of the cluster from the board (Supplementary Video 9). The resulting displacements at the tip for vertical shaking and horizontal shaking are in agreement with our hypothesis that differential normal strain gradients drive adaptation (Fig. 4c and Supplementary Video 10).

Our study has shown how dynamic loading of honeybee swarm clusters leads to mechanical adaptation wherein the cluster spreads out in response to repeated shaking that induced sufficiently large gradients in the relative displacements between individuals. We show that this adaptive morphological response increases the mechanical stability of the cluster. A computational model of the bee cluster treated as an active mechanical assemblage suggests that the active behavioural response of bees to local strain gradients can drive bee movement from regions of low strain to those of high strain and cause the cluster to flatten. This behavioural response improves the collective stability of the cluster as a whole via a reversible shape change, at the expense of increasing the time-averaged mechanical burden experienced by the individual.

Reporting Summary. Further information on experimental design is available in the Nature Research Reporting Summary linked to this article.

Data availability. The data that support the plots within this paper and other findings of this study are available from the corresponding author upon request.

Received: 26 September 2017; Accepted: 20 July 2018;
Published online: 17 September 2018

References

1. Seeley, T. D. *Honeybee Democracy* (Princeton Univ. Press, Princeton, NJ, 2010).
2. Anderson, C., Theraulaz, G. & Deneubourg, J. L. Self-assemblages in insect societies. *Insectes Soc.* **49**, 99–110 (2002).
3. Tennenbaum, M., Liu, Z., Hu, D. & Fernandez-Nieves, A. Mechanics of fire ant aggregations. *Nat. Mater.* **15**, 54–59 (2015).
4. Foster, P. C., Mlot, N. J., Lin, A. & Hu, D. L. Fire ants actively control spacing and orientation within self-assemblages. *J. Exp. Biol.* **217**, 2089–2100 (2014).
5. Mlot, N. J., Tovey, C. A. & Hu, D. L. Fire ants selfassemble into waterproof rafts to survive floods. *Proc. Natl Acad. Sci. USA* **108**, 7669–7673 (2011).
6. Mlot, N., Tovey, C. & Hu, D. Dynamics and circularity of large ant rafts.*Commun. Integr. Biol.* **5**, 590–597 (2012).
7. Peeters, C. & De Greef, S. Predation on large millipedes and self-assembling chains in *Leptogenys* ants from Cambodia. *R. Soc. Open Sci.* **4**, 471–477 (2015).
8. Jackson, W. B. Microclimatic patterns in army ant bivouacs. *Ecology* **38**, 276–285 (1957).
9. Phonekeo, S., Mlot, N., Monaenkova, D., Hu, D. L. & Tovey, C. Fire ants perpetually rebuild sinking towers. *R. Soc. Open Sci.* **4**, 170475 (2017).
10. Reid, C. R. et al. Army ants dynamically adjust living bridges in response to a cost-benefit trade-off. *Proc.Natl Acad. Sci. USA* **112**, 15113–15118 (2015).
11. Zitterbart, D. P., Wienecke, B., Butler, J. P. & Fabry, B. Coordinated movements prevent jamming in an emperor penguin huddle. *PLoS ONE* **6**, e20260 (2011).
12. Heinrich, B. Energetics of honeybee swarm thermoregulation. *Science* **212**, 565–566 (1981).
13. Ocko, S. A. & Mahadevan, L. Collective thermoregulation in bee clusters. *J. R. Soc. Interface* **11**, 20131033 (2013).
14. Gilbert, C., Robertson, G., Lemaho, Y., Naito, Y. & Ancel, A. Huddling behavior in emperor penguins: Dynamics of huddling. *Physiol. Behav.* **88**, 479–488 (2006).
15. Cully, S. M. & Seeley, T. D. Self-assemblage formation in a social insect: the protective curtain of a honey bee swarm. *Insectes Soc.* **51**, 317–324 (2004).
16. Hedrick, T. L. Software techniques for two- and three-dimensional kinematic measurements of biological and biomimetic systems. *Bioinsp. Biomim.* **3**, 034001 (2008).
17. Bahar, I., Lezon, T. R., Bakan, A. & Shrivastava, I. H. Normal mode analysis of biomolecular structures: functional mechanisms of membrane proteins. *Chem. Rev.* **110**, 1463–1497 (2010).
18. Persat, A. et al. The mechanical world of bacteria. *Cell* **161**, 988–997 (2015).

Acknowledgements

This work was supported by funding from the US NSF PoLS grant 1606895. We thank the Mahadevan laboratory for discussions and comments.

Author contributions

O.P., J.M.P. and L.M. conceived of the research study; O.P., J.M.P., M.K.S. and L.M. designed the experiments, O.P., J.M.P. and M.K.S. performed the experiments; O.P. analysed the data with the help of J.M.P; O.P. and L.M. conceived of the behavioural rule and designed the simulations; O.P. carried out the simulations; O.P., J.M.P. and L.M. wrote the paper; L.M. supervised the project.

Competing interests

The authors declare no competing interests.

Additional information

Supplementary information is available for this paper at https://doi.org/10.1038/s41567-018-0262-1.

Reprints and permissions information is available at www.nature.com/reprints.

Correspondence and requests for materials should be addressed to L.M.

Publisher's note: Springer Nature remains neutral with regard to jurisdictional claims in published maps and institutional affiliations.

nature physics

SUPPLEMENTARY INFORMATION

https://doi.org/10.1038/s41567-018-0262-1

In the format provided by the authors and unedited.

Collective mechanical adaptation of honeybee swarms

O. Peleg[1,4], J. M. Peters[2,4], M. K. Salcedo[2] and L. Mahadevan[1,2,3]*

[1]Paulson School of Engineering and Applied Sciences, Harvard University, Cambridge, MA, USA. [2]Department of Organismic and Evolutionary Biology, Harvard University, Cambridge, MA, USA. [3]Department of Physics, Kavli Institute for NanoBio Science and Technology, Harvard University, Cambridge, MA, USA. [4]These authors contributed equally: O. Peleg, J. M. Peters. *e-mail: lmahadev@g.harvard.edu

Collective mechanical adaptation of honeybee swarms

O. Peleg[1*], J.M. Peters[2*], M.K. Salcedo[2], L. Mahadevan, [1,2,3,†]

[1]Paulson School of Engineering and Applied Sciences,

[2]Department of Organismic and Evolutionary Biology,

[3]Department of Physics, Kavli Institute for NanoBio Science and Technology,

Wyss Institute for Biologically Inspired Engineering,

Harvard University, Cambridge, MA 02138, USA

[*]Equal contribution

[†]Corresponding author: Lmahadev@g.harvard.edu

Supplementary Information

Contents

A Experimental Methods

A.1 Study site.

All clusters were studied at Harvard University, Concord Field Station, Bedford, Massachusetts (42°30N, 72°10W).

A.2 Cluster preparation.

Animal research was conducted in accordance with the institutional animal care and use protocols of Harvard University. All of the clusters studied were artificial clusters were bought from honeybee suppliers (New England Beekeeping LTD, and Gold Star bees LTD), where the colony (10,000 worker/drone bees and a queen) is confined in a wooden box. Bees were a mix of Russian, Italian, and Carniolan bees. Clusters were prepared by separating the queen from the rest of the colony. The queen is placed in a small queen cage (3.2 x 10.0 x 1.6 cm). Next, the cluster box was opened and the queen (still in her own cage) was fastened to a cluster mount at position $U_i = V_i = W_i = 0$. The worker bees were then shaken onto the base of the mount whereupon they clustered around their queen.

A.3 Apparatus.

To analyze the mechanisms of mechanical stress adaptation, the clusters were mounted on a cluster mount (see Fig. 1B and Fig. 1A,B) which consists of a horizontal wooden board. The board was controlled by a motor (purchased from Applied Motion) that produced periodic movement in the horizontal or vertical axis at different frequencies and forces. The shape of the cluster was recorded via cameras (Logitech C270) positioned at three orthogonal locations (front, bottom, and side). Positions of individual bees were recorded using a high-speed frontal camera (SA3, Fastec Imaging) recording at 500 fps, and an $8-$megapixel iSight camera recording at 240 fps. Ambient temperature was recorded using a digital thermometer (A150Q Tech Instrumentation) that was fixed to the cluster mount, 2 cm above the clustered bees. Forces were measured using an accelerometer (SparkFun ADXL335) mounted on the wooden board.

A.4 Procedure.

A trial recording lasted 60 minutes, where shaking was applied for 30 minutes, and then no shaking was applied for additional 30 minutes. Equilibration period of 1 hour was applied within trials. During this time, the bees were fed ad libitum with a sugar solution (1:1 by volume, granulated sucrose: liquid water) by spraying it onto the cluster with a squirt bottle. Unless stated otherwise, single shaking response was recorded before the trial, and after 30 minutes. The responses to each mechanical shaking condition were replicated three times. Experiments were performed at 22 ± 2°C.

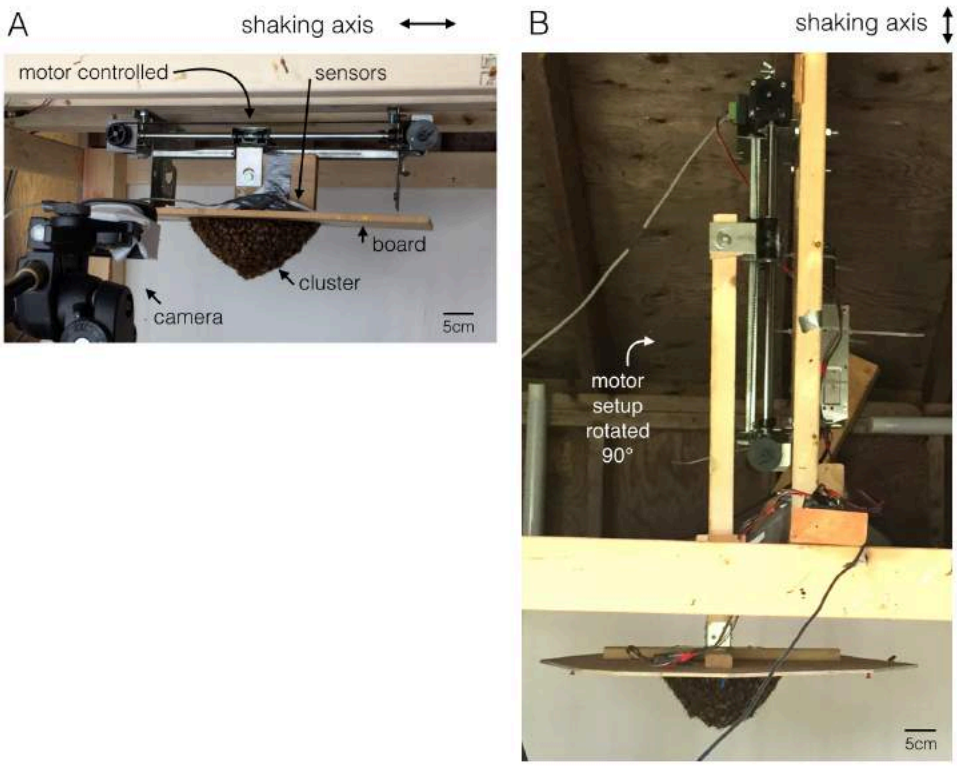

Figure 1: Experimental Setup: A) Horizontal shaking B) Vertical shaking. For the vertical shaking, the motor setup was rotated 90° to produce movement along the z axis.

A.5 Video analysis.

The shape of the cluster was extracted using the image analysis tool box of MATLAB 2016a. In particular, the base area, $A(t)$ was identified using image segmentation with a threshold value to turn the gray-scale image into a binary image. The number of pixels belonging to the base segment were translated to area using the pixel to cm^2 conversion via a calibration object. Individual honeybee positions were digitized using a freely available MATLAB application, DLTdv5 (***?***).

B Continuous vs. Discontinous Shakings

The measured accelerations during shaking events were recorded using an accelerometer mounted on the wooden board, and are shown in Fig. 2A, and Fig. 2B, for periodic and discontinuous shaking, respectively.

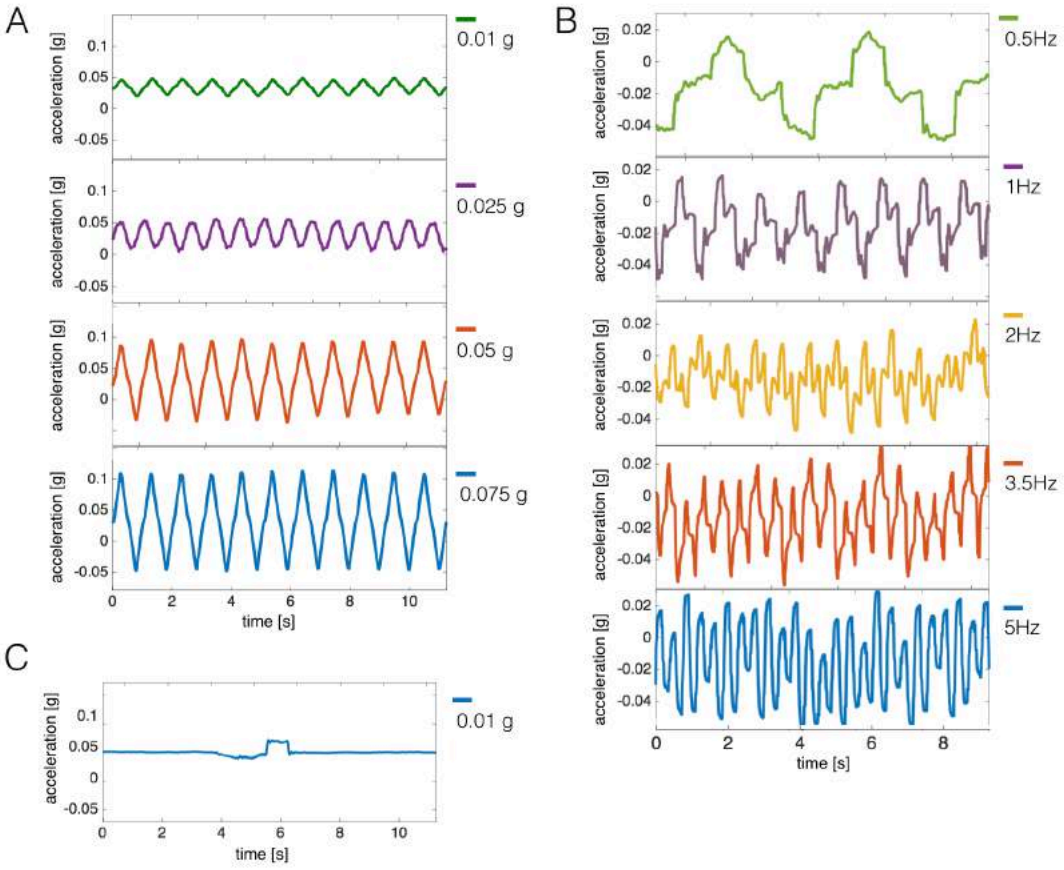

Figure 2: Mechanical Shaking Signals. A) Continuous shaking in which the frequency is kept constant and the acceleration is modified. B) Discontinuous shaking in which the acceleration is kept constant and the frequency is modified. C) A single sharp shake. Maximal acceleration or frequency values for each shaking signal appear in the legend.

Trial	Swarm	Stimulus type	Intensity	Direction	Date
1	1	discontinous	2 Hz	horizontal	23-Apr-15
2	1	discontinous	5 Hz	horizontal	23-Apr-15
3	1	discontinous	0.5 Hz	horizontal	24-Apr-15
4	1	discontinous	1 Hz	horizontal	24-Apr-15
5	1	discontinous	2 Hz	horizontal	24-Apr-15
6	1	discontinous	3.5 Hz	horizontal	24-Apr-15
7	1	discontinous	1 Hz	horizontal	25-Apr-15
8	1	discontinous	3.5 Hz	horizontal	25-Apr-15
9	1	discontinous	0.5 Hz	horizontal	26-Apr-15
10	1	discontinous	5 Hz	horizontal	26-Apr-15
11	1	discontinous	3.5 Hz	horizontal	26-Apr-15
12	1	discontinous	0.5 Hz	horizontal	27-Apr-15
13	1	discontinous	5 Hz	horizontal	27-Apr-15
14	1	discontinous	1 Hz	horizontal	27-Apr-15
15	1	discontinous	2 Hz	horizontal	27-Apr-15
16	2	continuous	0.075 g	vertical	10-Jun-15
17	2	continuous	0.1 g	vertical	10-Jun-15
18	2	continuous	0.075 g	vertical	10-Jun-15
19	2	continuous	0.075 g	vertical	11-Jun-15
20	2	continuous	0.1 g	vertical	11-Jun-15
21	2	continuous	0.025 g	horizontal	11-Jun-15
22	2	continuous	0.025 g	horizontal	11-Jun-15
23	2	continuous	0.01 g	horizontal	11-Jun-15
24	2	continuous	0.075 g	horizontal	12-Jun-15
25	2	continuous	0.025 g	horizontal	12-Jun-15
26	2	continuous	0.01 g	horizontal	12-Jun-15
27	2	continuous	0.075 g	horizontal	12-Jun-15
28	2	continuous	0.01 g	horizontal	12-Jun-15
29	2	continuous	0.075 g	horizontal	13-Jun-15
30	2	continuous	0.05 g	horizontal	13-Jun-15
31	2	continuous	0.05 g	horizontal	13-Jun-15
32	2	continuous	0.05 g	horizontal	13-Jun-15
33	2	continuous	0.025 g	horizontal	13-Jun-15
34	2	continuous	0.05 g	horizontal	13-Jun-15
35	2	continuous	0.025 g	vertical	15-Jun-15
36	2	continuous	0.05 g	vertical	15-Jun-15
37	2	continuous	0.025 g	vertical	16-Jun-15
38	2	continuous	0.025 g	vertical	16-Jun-15
39	2	continuous	0.05 g	vertical	16-Jun-15
40	2	continuous	0.05 g	vertical	16-Jun-15

Table 1: A description of the experimental trials, the particular swarm used (swarm 1 or swarm 2), the stimulus type (continuous or discontinous), intensity (frequency or acceleration), direction (horizontal or vertical) and the date they were performed.

C Statistical Tests

In this section we describe a series of statistical tests we perform to compare the observed experimental results across the varied experimental parameters.

We consider the time series of the ratio of the contact area of the base of the cluster divided by its original area $A(t)/A(0)$ as a function of time. We calculated the Pearson correlation coefficient between the time series of the continuous shaking, the horizontal and vertical case, for intensities 0.025g, 0.050g, and 0.075g. P–values for testing the hypothesis that there is no relationship between the observed time series (null hypothesis) are summarized in Table S3. This shows that all pairs of horizontal trials are significantly different, all pairs of vertical trials are not significantly different ($p < 0.05$). At low shaking intensities (0.025 g), the horizontal and vertical results are not significantly different, as in both cases the swarm doesn't flatten. As the intensity increases the horizontal and vertical results differ significantly $p < 0.01$ (for the 0.05 intensity) and $p < 0.001$ (for the 0.075 intensity).

		Horizontal			Vertical		
		0.025g	0.050g	0.075g	0.025g	0.050g	0.075g
Horizontal	0.025g	1	$p < 0.001^{***}$	$p < 0.001^{***}$	0.51	0.81	$p < 0.001^{***}$
	0.050g		1	$p < 0.001^{***}$	0.26	0.02^{**}	$p < 0.001^{***}$
	0.075g			1	0.75	0.01^{**}	$p < 0.001^{***}$
Vertical	0.025g				1	0.09^{*}	0.11
	0.050g					1	0.11
	0.075g						1

Table 2: P–values for testing the hypothesis that there is no relationship between the observed time series of the cluster divided by its original area ($A(t)/A(0)$). Significant p–values are highlighted via asterisk: $p < 0.1(^{*})$, $p < 0.05(^{**})$, and $p < 0.001(^{***})$.

D Numerical Model

Each honeybee is modeled as a $3D$ spherical particle of diameter a. Clusters at time $t = 0$ consisted of 1000 bees connected by linear springs arranged in a face centered lattice over a volume defined by a half-ellipsoid volume at different aspect ratios (i.e. different L_z/L_x values, as defined in Fig. **??**A). The board is represented as an additional layer of bees that serve as a physical non-permiable barrier. Their position is fixed as the position of the board $\overrightarrow{r_b(t)} = [U_b, V_b, W_b]$, and they are not subjected to Newton's equation of motion.

The rest of the bees (not represented on the board) experience three types of forces in the simulation. The first is the truncated Lennard Jones (LJ) defined as:

$$F^{\mathrm{LJ}}(\|\vec{r}\|) = \begin{cases} \dfrac{12\epsilon}{a}\left[\left(\dfrac{a}{\|\vec{r}\|}\right)^{13} - \left(\dfrac{a}{\|\vec{r}\|}\right)^{7} - \left(\dfrac{a}{\|\vec{r_{\mathrm{cutoff}}^{\mathrm{LJ}}}\|}\right)^{13} + \left(\dfrac{a}{\|\vec{r_{\mathrm{cutoff}}^{\mathrm{LJ}}}\|}\right)^{7}\right]\hat{r} & \|\vec{r}\| \leq r_{\mathrm{cutoff}}^{\mathrm{LJ}} \\ 0 & \mathrm{o/w} \end{cases} \tag{1a}$$

where $\vec{r}$ is the vector connecting the centers of the two particles; ϵ is the amplitude of the LJ potential; the force is truncated at the cutoff so that $F^{\mathrm{LJ}}(r_{\mathrm{cutoff}}^{\mathrm{LJ}}) = 0$. The second force is a spring force defined as:

$$F^{\mathrm{s}}(\|\vec{r}\|) = \begin{cases} k(\|\vec{r}\| - a)\hat{r} & \|\vec{r}\| < r_{\mathrm{cutoff}}^{\mathrm{s}} \\ 0 & \mathrm{o/w} \end{cases} \tag{2a}$$

where k is the spring coefficient. The third force is gravity, defined as:

$$F^{\mathrm{g}} = -mg\hat{y} \tag{3}$$

where g is the gravitational constant and m is the mass of a particle.

D.1 Normal modes.

To characterize the frequency of the lowest mode of the cluster, we perform Normal Mode Analysis (NMA) (***?***) on clusters of different aspect ratios. The free motion described by the normal modes takes place at fixed frequencies that depend on its structure, materials and boundary conditions. In this context, the lower the frequency, the less energy it takes to invoke its associated mode of motion and thus more likely to occur.

We force the top layer of bees to remain stationary. We assume small deformations of the network ($X_i << 1$) and Taylor expand the potential V. We take into consideration elements

up to power 2 of X_i, where X_i is the length of spring i minus its equilibrium length. The corresponding force on particles connected by spring i is:

$$F_i = \nabla_i V = \left(\frac{\partial^2 V}{\partial^2 X_i}\right) X_i + \sum_{j \neq i} \left[\left(\frac{\partial^2 V}{\partial X_i X_j}\right) X_j\right] \tag{4}$$

The harmonic potential of the spring connecting particles i and j is defined as:

$$V_{i,j} = \frac{1}{2} k \left(\left[(X_j - X_i)^2 + (Y_j - Y_i)^2 + (Z_j - Z_i)^2\right]^{1/2} - a\right)^2 \tag{5}$$

where X_i and X_j are the $x-$positions of particle i and j, respectively; Y_i and Y_j are the $y-$positions of particle i and j, respectively; Z_i and Z_j are the $z-$positions of particle i and j, respectively; a is the equilibrium length of the spring and k is the spring coefficient. In the general case of N particles connected by M springs in a $3D$ system, the second derivatives of the overall potential are organized in the $3N \times 3N$ Hessian matrix $\mathbb{H}$. $\mathbb{H}$ is composed of $N \times N$ super–elements of size 3×3, i.e. ,

$$\mathbb{H} = \begin{pmatrix} \mathbf{H}_{1,1} & \mathbf{H}_{1,2} & \cdots & \mathbf{H}_{1,n} \\ \mathbf{H}_{2,1} & \mathbf{H}_{2,2} & \cdots & \mathbf{H}_{2,n} \\ \vdots & \vdots & \ddots & \vdots \\ \mathbf{H}_{n,1} & \mathbf{H}_{n,2} & \cdots & \mathbf{H}_{n,n} \end{pmatrix} \tag{6}$$

where

$$\mathbf{H}_{ij} = \begin{pmatrix} \frac{\partial^2 V}{\partial X_i X_j} & \frac{\partial^2 V}{\partial X_i Y_j} & \frac{\partial^2 V}{\partial X_i Z_j} \\ \frac{\partial^2 V}{\partial Y_i X_j} & \frac{\partial^2 V}{\partial Y_i Y_j} & \frac{\partial^2 V}{\partial Y_i Z_j} \\ \frac{\partial^2 V}{\partial Z_i X_j} & \frac{\partial^2 V}{\partial Z_i Y_j} & \frac{\partial^2 V}{\partial Z_i Z_j} \end{pmatrix} \tag{7}$$

The equation of motions can then be written as $\mathbf{F} = \mathbb{H} \cdot \mathbf{D}$, where

$$\mathbf{D} = (X_1, Y_1, Z_1, X_2, Y_2, Z_2 \cdots X_n, Y_n, Z_n) \tag{8}$$

is vector of all X, Y and Z positions of particles in the system. We solve $\mathbf{M}\ddot{\mathbf{D}} - \mathbb{H}\mathbf{D} = 0$ by converting it to the following Eigen value problem of the Hessian matrix: $(\mathbb{H} - \lambda \mathbf{I}) = 0$, where λ is a set of the Eigen values and I is a unit matrix. The Eigen values represent frequencies of motion, and the Eigen vectors represent displacement of all particles in the system.

As expected, the pendular motion is the lowest frequency normal mode of the elongated cluster (Fig. 3). It is the most likely to occur naturally (under the NMA assumptions) and thus also the most relevant stimulus the honeybees experience. The frequency associated with the pendular mode increases monotonically as a function of the aspect ratio of the cluster, L_z/L_x. Therefore, modulation of the aspect ratio suffices to reduce the strain.

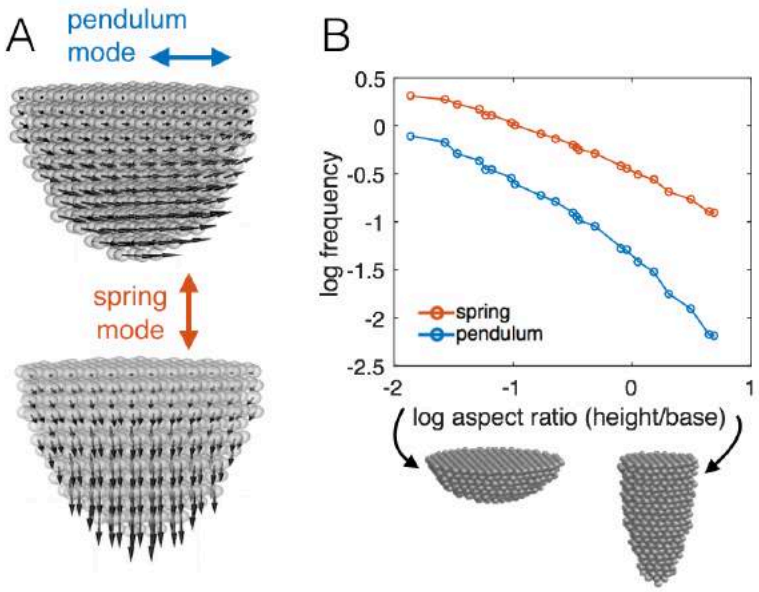

Figure 3: Normal mode analysis show that the primary deformation modes are associated with spring and pendulum modes - consistent with experimental observations. A) Illustration of the displacements associated with pendulum (top) and spring (bottom) modes. B) The normal mode's frequencies as a function of aspect ratio.

D.2 Passive simulations to extract local strains.

To extract the local strains, the positions of the top bees were manipulated to produced periodic movement in the horizontal or vertical axis at different frequencies and forces (similarly to the experiments, e.g., Fig. **??**C). The rest of the bees obey the Langevin equations of motion: $\dot{\mathbf{r}}_i = \mathbf{p}_i/m$, and $\dot{\mathbf{p}}_i = -\zeta \mathbf{p}_i + \mathbf{f}_i$, where $\dot{\mathbf{r}}_i$ is the velocity of particle i; ζ is the friction; $\mathbf{f}_i$ is the force acting on the particle. The bees experience all three forces mentioned above: F^{LJ}, F^{s}, and F^{g} with associated parameters listed in Table S2.

Local instantaneous strains were measured relative to a reference configuration in the absence of shaking at $t = 0$, as shown in Fig. **??**A–C and Fig. 3, according to the definitions in the main text.

Time integrated local strains presented in Fig. **??**D–E, Fig. 3 and Fig. 4 were defined using a modified instantaneous signal:

$$\delta l_i^t = \sqrt{\left(\sum_{\forall j \in i} l_{ij}^x(t+1) - l_{ij}^x(t)\right)^2 + \left(\sum_{\forall j \in i} l_{ij}^y(t+1) - l_{ij}^y(t)\right)^2} \tag{9}$$

for each neighbor j of particle i that is connected via spring. The time integrated signal is defined as $\widetilde{\delta l_i^t} = \sum_{\tilde{t}=t-T_w}^{t} \delta l_i^{\tilde{t}} \times dt$, where T_w is the time duration in which the signal is integrated and is chosen to be the period of the shaking.

D.3 Active stochastic simulations to follow active behavior

We performed a Stochastic Dynamics simulations to follow the active behavior of bees. The bees obey the over–damped equations of motion: $\dot{\mathbf{r}}_i = -\mathbf{f}_i + \tilde{\mathbf{r}}_i$, where $\tilde{\mathbf{r}}_i$ is a Gaussian random number with mean zero and variance η. $\mathbf{f}_i$ is the force acting on the particle which include F^{LJ}, F^{s}, and an active force F^{active}, with associated parameters listed in Table S2.

When $\widetilde{\delta l_i^t} > \widetilde{\delta l_{iC}^t}$ the honeybee becomes active, and experiences an additional force in the direction of the time integrated negative normal stain gradient (i.e. the active force is directed toward a higher local strain):

$$F^{\mathrm{active}} = -f^{\mathrm{active}} \overrightarrow{\widetilde{\delta l_i^t}} \tag{10}$$

The direction, $\overrightarrow{\widetilde{\delta l_i^t}}$, is calculated as:

$$\overrightarrow{\widetilde{\delta l_i^t}} = \left(\sum_{\tilde{t}=t-T_w}^{t} \delta l_i^x(\tilde{t}) \times dt \right) \widehat{x} + \left(\sum_{\tilde{t}=t-T_w}^{t} \delta l_i^y(\tilde{t}) \times dt \right) \widehat{y} \tag{11}$$

where the instantaneous signal is defined as $\delta l_i^x(t) = \sum_{\forall j \in i} \delta l_{ij} \widehat{l_{ij}^x(t)}$, $\delta l_i^y(t) = \sum_{\forall j \in i} \delta l_{ij} \widehat{l_{ij}^y(t)}$, $\delta l_{ij} = \left| \left| \overrightarrow{l_{ij}(t)} \right| - \left| \overrightarrow{l_{ij}(0)} \right| \right|$.

If an active honeybee has less than 6 spring bonded interactions it would have a tendency to move towards one of its neighbors and could lead to pathological expansion of cavities in the cluster. To prevent this, we allow bees to become active only if they have 6 spring bonded interactions.

			Unitless Value		
Parameter	Description	Type	Passive	Active	NMA
a	honeybee diameter	length	$2^{1/6} \sim 1.122$	$2^{1/6} \sim 1.122$	$2^{1/6} \sim 1.122$
k	spring coefficient	force/length	5×10^2	5×10^2	5×10^2
ϵ	Lennard-Jones (LJ) amplitude	length	1	2×10^2	–
g	gravitational coefficient	force	10^{-2}	–	–
η	amplitude of stochastic noise	length	0	2×10^{-2}	–
ζ	friction	force	5	–	–
f^{active}	active force	force	–	2.5×10^2	–
$r^{\text{LJ}}_{\text{cutoff}}$	cutoff for LJ force	force	a	3.5	–
$r^{\text{s}}_{\text{cutoff}}$	cutoff for spring force	length	$\inf$	1.2	–
dt	time integration constant	time	3×10^{-2}	5×10^{-5}	–
$\widetilde{\delta l^t_{iC}}$	local strain threshold to become active	–	–	4×10^{-3}	–

Table 3: Simulation parameters values for both the passive and active simulations described in section D, as well as the Normal Mode Analysis (NMA).

E Response to Horizontal vs. Vertical Shakings

To test the differential strain hypothesis, we simulate the active model and compare the response of the cluster to horizontal and vertical shaking. Both the maximal instantaneous normal strain (Fig. 4) as well as the integrated normal strain (Fig. 4) are higher in response to a horizontal shaking. Therefore, there exists an activation threshold $\widetilde{\delta l_{iC}^t}$, such that most bees will not respond to vertical shaking but would respond to horizontal shaking. Indeed, we see that in this case the cluster shape remains approximately constant when vertical shaking are applied (Fig. 4C–D), while the the bees adapt by spreading themselves into a squatter conical form when horizontal shaking are applied (Fig. 4A–B).

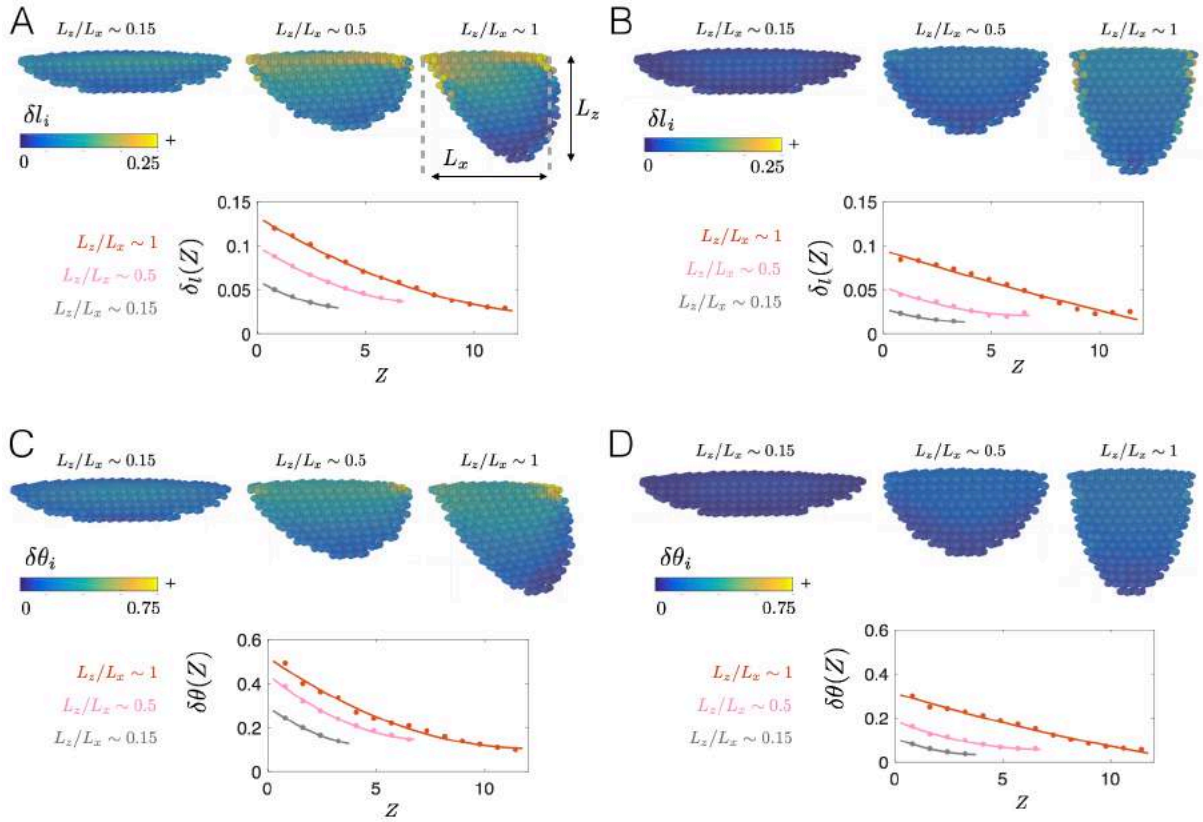

Figure 4: Passive simulations of a 3D clusters. A) Clusters of different aspect ratios (L_z/L_x), shown at an extreme end of an oscillation associated with largest normal strains. Colors represent the local normal strain of each honeybee δl_i. Elongated clusters (on the right) experience a larger deformation at the tip of the cluster, while squat clusters (on the left) experience low deformations. Fountain plots show the mean normal strain ($\delta l(Z)$) as a function of the distance from the base, Z, and aspect ratio L_z/L_x. B) Same as A for a vertical shaking. C,D) same as A,B for the mean shear strain ($\delta\theta(Z)$).

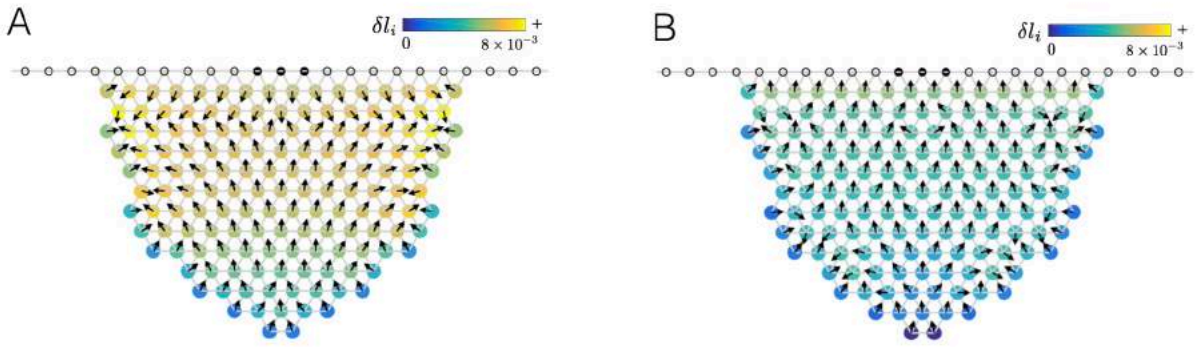

Figure 5: Local integrated normal strains resulting from one shaking period in active stochastic simulations . A) When horizontal shaking is applied. B) When vertical shaking is applied. Colors represent the local integrated signal, $\widetilde{\delta l_i^t}$, and arrows represent the direction towards higher local signal.

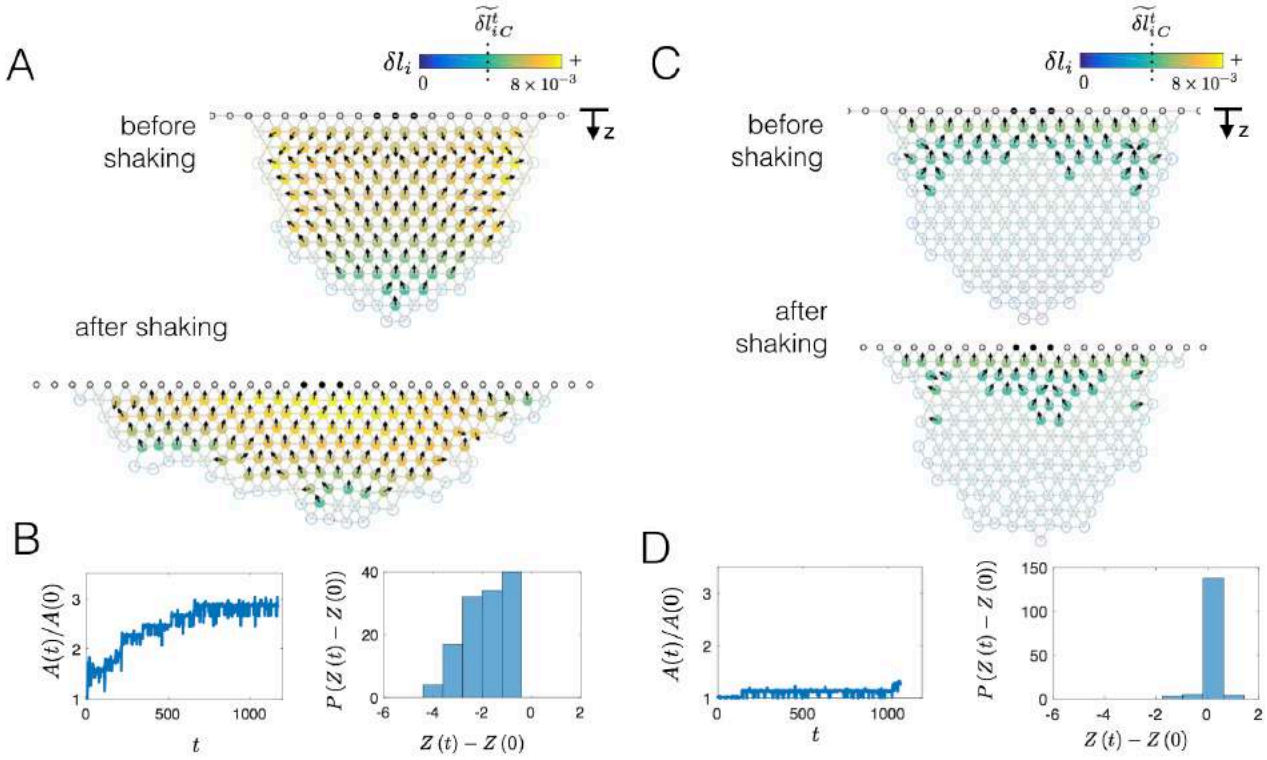

Figure 6: Active stochastic simulations in which the bees monitor their local deformation and follow a local rule in which once the deformation is larger than a certain threshold, the honeybee has a bias to move toward a region of higher local deformation. In agreement with experimental results, spreading occurs during horizontal shaking (A) but not during vertical shaking (C), in agreement with the experimental results. Colors represent the local integrated signal, $\widetilde{\delta l_i^t}$, and arrows represent the direction towards higher local signal. B,D) The relative base area as a function of time is similar to the results of experiments, with the probability distribution function of vertical displacement shows a net negative response, i.e. bees move upwards on average, for horizontal and vertical shaking respectively.

F Description of Supplementary Movies

F.1 Movie S1 Honeybee cluster in the wind

Feral cluster at the study cite, in the presence of wind. Acquisition and playback frame rate: 3×10^2 fps.

F.2 Movie S2 Time-lapse of horizontal shaking experiment

A time lapse video showing the shape change of the cluster during a horizontal shaking trial. Top panel: front view; Bottom panel: bottom view. Acquisition frame rate: 5×10^{-2} fps. Playback sped up $\times 600$. The applied shaking is discontinuous, in which the acceleration is kept constant and the frequency was set to 5Hz (see signal in Fig. 2B).

F.3 Movie S3 Before/after horizontal shaking experiment - response to continuous shaking

High–speed video of a single sharp horizontal shaking. Top: the cluster before a shaking trial. Bottom: the cluster after a shaking trial of continuous shaking with an acceleration of 0.075g. Acquisition frame rate: 5×10^2 fps. Playback slowed down $\times 16$.

F.4 Movie S4 Before/after horizontal shaking experiment - response to a single sharp shake

High–speed video of a single sharp horizontal shaking. Top: the cluster before a shaking trial. Bottom: the cluster after a shaking trial of continuous shaking with an acceleration of 0.075g. Acquisition frame rate: 5×10^2 fps. Playback slowed down $\times 16$.

F.5 Movie S5 Tracking individual bees during horizontal shaking experiment

High–speed video of the first 5 minutes of a horizontal shaking trial where the camera was mounted to the board. The shaking applied was continuous with an acceleration of 0.075g.

Acquisition frame rate: 2.4×10^2 fps. Playback sped up $\times 60$. Each tracked honeybee is highlighted in a different color. Trajectories of individual bees show that when the cluster spreads out, surface bees move upwards.

F.6 Movie S6 Passive simulations to extract local strains

Dynamics simulations of a 3D clusters of different aspect ratios (L_z/L_x). Colors represent the local normal strain of each honeybee δl_i. The movies illustrate the following:

1. Elongated clusters experience a larger deformation (δl_i) at the tip of the cluster than at the base, while squat clusters experience low deformations everywhere.
2. In comparison to horizontal shaking, vertical shaking result in a minute δl_i.

F.7 Movies S7–8 Active simulations

Simulation of an active cluster in which the bees monitor their local deformation and follow a local rule in which once the deformation is larger than a certain threshold, the honeybee has a bias to move toward a region of higher local deformation. This leads to spreading when horizontal shaking are applied and no spreading when vertical shaking are applied, in agreement with the experimental results. Colors represent the local integrated signal, $\widetilde{\delta l_i^t}$, and arrows represent the direction towards higher local signal. The accelerations applied to the board $\partial^2 U_b/\partial^2 t$, and $\partial^2 W_b/\partial^2 t$, are shown at the upper right corner of the movies.

Movie S7 A typical event of horizontal shaking in which the local signal is integrated to $\widetilde{\delta l_i^t}$, followed by active response of the cluster to 35 horizontal shaking events.

Movie S8 A typical event of vertical shaking in which the local signal is integrated to $\widetilde{\delta l_i^t}$, followed by active response of the cluster to 35 vertical shaking events.

F.8 Movie S9 Honeybee cluster breakage

Video of cluster breakage during a vertical shaking trial of continuous shaking with an acceleration of 0.1g. Acquisition frame rate: 3×10^2 fps.

F.9 Movie S10 Before/after vertical shaking experiment - response to a single sharp shake

High–speed video of a single sharp vertical shaking. Top: the cluster before a shaking trial. Bottom: the cluster after a shaking trial of continuous shaking with an acceleration of 0.075g. Acquisition frame rate: 3×10^2 fps. Playback slowed down $\times 16$.